

## Research Article

# Are impermeable curtains necessary for a groundwater contaminant remediation project?

Ming Guo<sup>1</sup>, Yun Yang<sup>2</sup>, Qian-kun Luo<sup>1\*</sup>, Ying-chun Li<sup>3</sup>, Hai-chun Ma<sup>1</sup>, Jia-zhong Qian<sup>1</sup>

<sup>1</sup> School of Resources and Environmental Engineering, Hefei University of Technology, Hefei 230009, China.

<sup>2</sup> Huai River Water Resources Commission, Bengbu 233001, Anhui Province, China.

<sup>3</sup> Public-welfare Geological Survey Management Center of Anhui Province & Geological Survey and Environmental Monitoring Center of Anhui Province, Hefei 230091, China.

**Abstract:** Constructing impermeable curtains to contain contaminant in aquifers is a costly and complex process that can impact the structure integrity of aquifer systems. Are impermeable curtains necessary for a groundwater contaminant remediation project? This study evaluates the necessity of impermeable curtains for groundwater contaminant remediation projects. Specifically, it considers remediation efforts based on the Pump and Treat (PAT) technique under various hydrogeological conditions and contaminant properties, comparing the total remediation cost and effectiveness. To further investigate, a multi-objective simulation and optimization model, utilizing the Multi-Objective Fast Harmony Search (MOFHS) algorithm, was employed to identify optimal groundwater remediation system designs that without impermeable curtains. Both a two-dimensional (2-D) hypothetical example and a three-dimensional (3-D) field example were used to assess the necessity of constructing impermeable curtains. The 2-D hypothetical example demonstrated that the installation of impermeable curtain is justified only when the dispersivity ( $\alpha_L$ ) of the contaminant reaches 100 meters. In most cases, particularly at sites with porosity ( $n$ ) under 0.3, alternative, more cost-effective, and efficient remediation strategies may be available, making impermeable barriers unnecessary. The optimization results of the 3-D field example further corroborate the conclusions derived from the 2-D hypothetical example. These findings provide valuable guidance for more scientifically informed, reasonable, and cost-effective groundwater contaminant remediation projects.

**Keywords:** Groundwater contaminant; Hydrogeological condition; Contaminant characteristics; Impermeable curtains; Simulation and optimization; PAT

Received: 23 Jul 2024/ Accepted: 28 Dec 2024/ Published: 27 Jun 2025

## Introduction

Water is essential for sustaining life (Rodell et al. 2009). According to the World Health Organization (WHO), water scarcity affects over 40% of the global population, which corresponds to over 2 billion people who lack access to adequate or clean water (Fu et al. 2014). Meanwhile, industrial and

urban activities have led to the widespread contamination of groundwater, posing significant risks to the health and well-being of millions of people worldwide (Vidic et al. 2013). Consequently, effective groundwater contaminant remediation is crucial for mitigating these adverse effects and ensuring access to safe drinking water.

Remediation cost and effects must be comprehensively evaluated before groundwater initiating any groundwater contaminant remediation project, irrespective of the remediation techniques utilized, due to the significant cost and time commitments involved in such efforts (Park, 2016). The use of impermeable curtains is a common method for controlling the occurrence and dispersion of aquifer contaminants. These curtains are particularly effective for sites that do not require further

\*Corresponding author: Qian-kun Luo, E-mail address: [QKLuo@hfut.edu.cn](mailto:QKLuo@hfut.edu.cn)

DOI: [10.26599/JGSE.2025.9280052](https://doi.org/10.26599/JGSE.2025.9280052)

Guo M, Yang Y, Luo QK, et al. 2025. Are impermeable curtains necessary for a groundwater contaminant remediation project?. Journal of Groundwater Science and Engineering, 13(3): 237-249.

2305-7068/© 2025 Journal of Groundwater Science and Engineering Editorial Office. This is an open access article under the CC BY-NC-ND license (<http://creativecommons.org/licenses/by-nc-nd/4.0>)

remediation measures, such as those with limited commercial value or those located far from residential areas and environmentally sensitive zones. However, for contaminated sites of high commercial value, or those near residential or environmentally sensitive areas, additional remediation efforts become essential. Historically, numerous groundwater contaminant remediation projects commenced with the installation of impermeable curtains, followed by subsequent remediation work, such as Pump and Treat (PAT) (Gao et al. 2019; Lyu et al. 2021; Wang et al. 2020; Yang et al. 2022). However, the cost of constructing impermeable curtains can range from several millions to tens of millions of CNY, depending on the scale of the contaminated area (Song, 2014). The construction process typically involves drilling and grouting, with materials such as cement, hot bitumen, coal slurry, modified clay, and polyurethane foam mortar being commonly used for grouting (Kim et al. 2017; Tang et al. 2023). Aside from altering the spatial structure and mechanical properties of the subsurface, the inclusion of cement or other materials during curtain construction may also introduce additional contaminants into the groundwater through leakage. Given these concerns, a critical question arises: Are impermeable curtains necessary for all groundwater contaminant remediation projects?

Generally, the transport of contaminant is controlled by hydrogeological conditions and characteristics of the contaminants at a site (Locatelli et al. 2019). The hydrogeological conditions of a contaminated site include factors such as the recharge, runoff, and discharge conditions of groundwater, the spatial structure of aquifers, and key hydrogeological parameters, such as hydraulic conductivity ( $K$ ), and porosity ( $n$ ). The characteristics of the contaminant include their adsorption, degradation, dispersivity, and diffusion, etc (Cao et al. 2019; Elango et al. 2012). When the runoff conditions and permeability of the aquifer at a contaminant remediation site are poor, and the contaminant's dispersivity and diffusion coefficients are low, the transport of contaminant through the aquifer will be slow. In such cases, it may not be necessary to incur the high costs of constructing impermeable curtains to control contaminant transport. Therefore, it is unwise to construct impermeable curtains without thoroughly considering the specific hydrogeological conditions and contaminant characteristics of the site. Moreover, the necessity of impermeable curtains should be evaluated by comparing the total remediation costs and effects with and with-

out their implementation.

The Multi-Objective Simulation and Optimization (MOSO) model method (Wu et al. 2005) is widely regarded as one of the most effective techniques for addressing optimization problems in groundwater contaminant remediation systems (Bader and Zitzler, 2011; Luo et al. 2016, 2014; Song et al. 2019, 2018; Wang et al. 2022; Yang et al. 2021). The MOSO model offers the advantages of strictly adhering to groundwater flow laws while simultaneously managing a set of constraints to identify optimal management strategies (Mattila and Virtanen, 2014). Therefore, in this study, the MOSO model method was employed to determine potential optimal designs for groundwater contaminant remediation systems without the construction of impermeable curtains.

The solution to a MOSO problem is a set of Pareto solutions (non-dominated solutions) in contrast to the single-objective optimization problem (Deb, 2001). Multi-Objective Evolutionary Algorithms (MOEAs) are effective tools for identifying Pareto solutions in optimization problems characterized by large decision spaces and conflicting objectives (Deb, 2001; Deb et al. 2002). Among these, the Multi-Objective Fast Harmony Search (MOFHS) algorithm stands out as a promising MOEA, ensuring the uniformity and integrity of the Pareto front in multi-objective optimization problems (Luo et al. 2020, 2016; Yang et al. 2018). Therefore, in this study, the MOFHS algorithm was employed to identify Pareto solutions of the MOSO model of optimal design of a groundwater remediation system without the construction of impermeable curtains.

In this study, we use the PAT technique as a case study to investigate the necessity of constructing impermeable curtains for groundwater contaminant remediation projects under various hydrogeological conditions and contaminant characteristics. Section 2 provides a comprehensive introduction to the calculation methods both with and without impermeable curtains. Section 3 presents the calculation results and a discussion of both the 2-D hypothetical and 3-D field problems. The study concludes with a summary of key findings.

## 1 Methods

### 1.1 Groundwater remediation with the construction of impermeable curtains

In this study, two types of aquifers, unconfined and confined aquifers, are considered to represent the

diverse hydrogeological properties of contaminated sites. The total cost ( $f_T$ ) of a groundwater contaminant remediation system based on the PAT technique with impermeable curtains generally consists of two components: The cost of the PAT system ( $f_{PAT}$ ) and the cost of constructing impermeable curtains ( $f_{CIC}$ ). The calculation formulas for  $f_{PAT}$ ,  $f_{CIC}$  and  $f_T$  under different hydrogeological conditions of the contaminant sites are as follows:

$$f_{PAT} = Qp_1 \tag{1}$$

$$f_{CIC} = 2PS_t p_2 \tag{2}$$

$$f_T = f_{PAT} + f_{CIC} \tag{3}$$

For confined aquifers:

$$Q = S(h_A - S_t)A + \mu AS_t \tag{4}$$

For unconfined aquifers:

$$Q = \mu Ah_A \tag{5}$$

Where:  $Q$  is the total pumping volume [ $L^3$ ];  $p_1$  and  $p_2$  represent the unit-price of contaminated water treatment using PAT [ $CNYL^{-3}$ ] and impermeable curtains construction [ $CNYL^{-2}$ ], respectively;  $P$  is the perimeter of the impermeable curtains [ $L$ ];  $A$  is the area of the impermeable curtains [ $L^2$ ];  $S_t$  is the thickness of aquifer [ $L$ ];  $S$  is the storage coefficient;  $h_A$  is the average groundwater head [ $L$ ];  $\mu$  is the specific yield.

## 1.2 Groundwater remediation without impermeable curtains

In this study, the cost and effectiveness of groundwater remediation without impermeable curtains are calculated using the MOSO model method based on the MOFHS algorithm. The MOSO model for groundwater remediation system consists of two primary components: Groundwater flow and transport simulation models and a multi-objective optimization model for the optimal design of the remediation systems (Luo et al. 2014). A detailed description of the MOSO model for optimal design of groundwater remediation system design, as well as the MOFHS algorithm, is provided in the following subsections.

### 1.2.1 Groundwater flow and transport simulation models

Based on the hydrogeological conceptual model of the study area, when the main direction of the anisotropic medium aligns with the coordinate axis, the 3-D groundwater flow in the porous medium can be represented by the following

partial differential equations (assuming constant groundwater density) (Warren et al. 2002):

$$\frac{\partial}{\partial x} \left( K_{xx} \frac{\partial H}{\partial x} \right) + \frac{\partial}{\partial y} \left( K_{yy} \frac{\partial H}{\partial y} \right) + \frac{\partial}{\partial z} \left( K_{zz} \frac{\partial H}{\partial z} \right) + W = S_s \frac{\partial H}{\partial t} \tag{6}$$

Where:  $K_{mm}$  ( $m = x, y, z$ ) represents the permeability coefficient tensor, with subscripts  $x, y, z$  corresponding to components in the respective directions [ $LT^{-1}$ ];  $H$  is the hydraulic head [ $L$ ];  $W$  is the volumetric flow rate of fluid sinks/sources per unit-volume of the aquifer [ $LT^{-1}$ ], representing the amount of water flowing into or out of the source;  $S_s$  is specific storage [ $L^{-1}$ ];  $t$  is time [ $T$ ].

The partial differential equation describing 3-D solute transport in groundwater is given by Zheng and Wang (1999):

$$\frac{\partial C}{\partial t} = \sum_{i=1}^3 \frac{\partial}{\partial i} \left( D_{ii} \frac{\partial C}{\partial x} \right) - \frac{\partial}{\partial i} (u_i C) + f \tag{7}$$

Where:  $C$  is the solute concentration [ $ML^{-3}$ ];  $D_{ii}$  is the component of hydrodynamic dispersivity coefficient in the  $i$ -direction [ $L^2T^{-1}$ ], where  $i = 1, 2,$  and  $3$  corresponds to  $x, y,$  and  $z,$  respectively;  $\mu_i$  is the component of actual flow rate of groundwater in the  $i$ -direction [ $LT^{-1}$ ];  $f$  is the concentration changes caused by chemical reactions or other factors [ $ML^{-3}T^{-1}$ ].

The flow and transport equations described in Eqs. (6)-(7), along with specific boundary and initial conditions, form the mathematical model for describing actual groundwater flow problems. In this study, the 3-D finite-difference groundwater flow code, MODFLOW (Harbaugh, et al. 2000), and its solute transport companion, MT3DMS (Zheng and Wang, 1999), are used as the flow and transport simulation models to predict the groundwater flow and contaminant plume distribution. The classical version of MODFLOW and MT3DMS are integrated as subroutines within the main optimization program to address the optimal design problem of the groundwater remediation system (Luo et al. 2014).

### 1.2.2 The multi-objective optimization model of groundwater remediation system

The mathematical expression of a general multi-objective optimization problem can be described as (Rao, 1979):

$$\min / \max y = F(x) = (f_1(x), f_2(x), \dots, f_k(x)) \tag{8}$$

subject to

$$g_i(x) \leq 0, i = 1, 2, \dots, M \tag{9}$$

$$h_i(\mathbf{x}) = 0, i = 1, 2, \dots, P \quad (10)$$

$$l_i \leq x_i \leq u_i, i = 1, 2, \dots, N \quad (11)$$

Where:  $\mathbf{y} = (y_1, y_2, \dots, y_k) \in \mathbf{Y}, y_i = f_i(\mathbf{x})$  is the  $i$ -th objective function in the  $k$ -th objective,  $\mathbf{Y}$  is the objective function space;  $\mathbf{x} = (x_1, x_2, \dots, x_n) \in X, \mathbf{x}$  is the  $n$ -dimensional decision variable vector, representing a solution vector,  $X$  is the set of feasible solutions, namely the feasible variable space, which is constrained by  $\mathbf{M}$  inequality (Eq. (9)) and  $\mathbf{P}$  equality (Eq. (10)),  $l_i$  and  $u_i$  represent the lower and upper limits of the  $i$ -th decision variable  $x_i$ , respectively.

In this study, the primary objectives of optimal design for a groundwater contaminant remediation system are:

1. Minimizing remediation costs.
2. Minimizing residual contaminant content in aquifers (quantitatively describing the remediation effect) at the end of the remediation period, subject to a set of constraints. The objective functions can be expressed as follows (Chang et al. 2007; Yang et al. 2021):

$$\min J_1 = \alpha_1 \sum_{i=1}^{N_w} w_i + \alpha_2 \sum_{i=1}^{N_w} w_i d_i + (\alpha_3 + \alpha_4) \sum_{i=1}^{N_w} \sum_{t=1}^{N_t} w_i |Q_i^t| \Delta t_t \quad (12)$$

$$\min J_2 = \left( \frac{mass_{end}}{mass_0} \right) \times 100\% \quad (13)$$

Where:  $J_1$  is the total remediation cost over the entire remediation period;  $\alpha_i (i = 1, 2, 3, 4)$  is the cost coefficient associated with well installation, well drilling, water pumping and contaminant treatment, respectively;  $N_w$  is the number of the pumping wells;  $w_i$  is a binary variable indicating whether well  $i$  is drilled ( $w_i = 1$ , drilled;  $w_i = 0$ , not drilled);  $d_i$  is the depth of well bore associated with well;  $N_t$  is the total number of management periods;  $Q_i^t$  is the pumping rate associated with well  $i$  during the  $t$ -th management period;  $\Delta t_t$  is the duration of the  $t$ -th management period;  $J_2$  is the residual contaminant content at the end of the remediation period;  $mass_{end}$  and  $mass_0$  are the total solute mass in the aquifer at the end and beginning of the remediation period, respectively.

The constraints of the optimization model in this study are as follows (Zheng and Wang, 2003):

$$\sum_{i=1}^{N_w} w_i \leq N_w \quad (14)$$

$$h_j^{\min} \leq h_j \leq h_j^{\max}, j = 1, 2, \dots, N_h \quad (15)$$

$$h_k^{out} - h_j^{\min} \geq \Delta h_k^{\min}, k = 1, 2, \dots, N_g \quad (16)$$

$$C_l^{\min} \leq C_l \leq C_l^{\max}, l = 1, 2, \dots, N_c \quad (17)$$

$$Q_i^{\min} \leq Q_i \leq Q_i^{\max}, i = 1, 2, \dots, N_w \quad (18)$$

$$C_m < C^* \quad (19)$$

Where: Eq. (14) limits the total number of wells to ensure that the actual number of wells drilled does not exceed the number of wells designated for optimization; Eq. (15) constrains the groundwater head at each constraint point  $j$  during the remediation period to lie between a specified lower limit ( $h_j^{\min}$ ) and upper limit ( $h_j^{\max}$ ), and  $N_h$  represents the total number of constraint point  $j$ ; Eq. (16) ensures that the difference between the upper and lower gradient hydraulic head at constraint point  $k$  is not less than the specified lower limit  $\Delta h_k^{\min}$ , and  $N_g$  is the total number of constraint point  $k$ ; Eq. (17) constrains the contaminant concentration at each location  $l$  to remain within the given lower limit ( $C_l^{\min}$ ) and upper limit ( $C_l^{\max}$ ) during the remediation period, and  $N_c$  is the total number of locations; Eq. (18) restricts the pumping rate for each well  $i$  to remain within the lower limit ( $Q_i^{\min}$ ) and upper limit ( $Q_i^{\max}$ ) during the remediation period; Eq. (19) ensures that the calculated concentration ( $C_m$ ) at any monitoring location does not exceed the maximum contaminant level ( $C^*$ ) within the area of compliance.

In multi-objective optimization models, as expressed in Eqs. (8)-(11), the term "Pareto solutions" or "non-dominant solutions" refers to the set of optimal solutions. A Pareto-optimal solution, or non-dominant solution, is defined by the absence of any alternative solution that can simultaneously improve all objectives. In essence, if  $x^* \in X$  and  $x^*$  stands as Pareto-optimal solutions, it implies that no other solution  $x \in X$ , such that  $F(x) < F(x^*)$ , exists in the decision variable space,  $X$  (Luo et al. 2012).

### 1.2.3 MOFHS

The MOFHS algorithm was developed by Luo et al. (2012) as an enhancement of the original Harmony Search (HS) algorithm (Zong Woo Geem et al. 2001). The improvements in MOFHS included the incorporation of niche Pareto domination ranking and fitness value sharing operations, which enable it to effectively identify Pareto solutions for multi-objective optimization problems (Luo et al. 2012; Yang et al. 2017). Additional features, such as the Pareto solution set filter and the elite individual preservation strategy, were integrated into MOFHS to ensure the diversity of

Pareto solutions and accelerate convergence speed to the true Pareto fronts. For further details, refer to Luo et al. (2012).

Fig. 1 illustrates the flowchart of the MOSO model for the optimal design of groundwater remediation systems using the MOFHS algorithm. The process consists of five primary steps, as outlined by Luo et al. (2012):

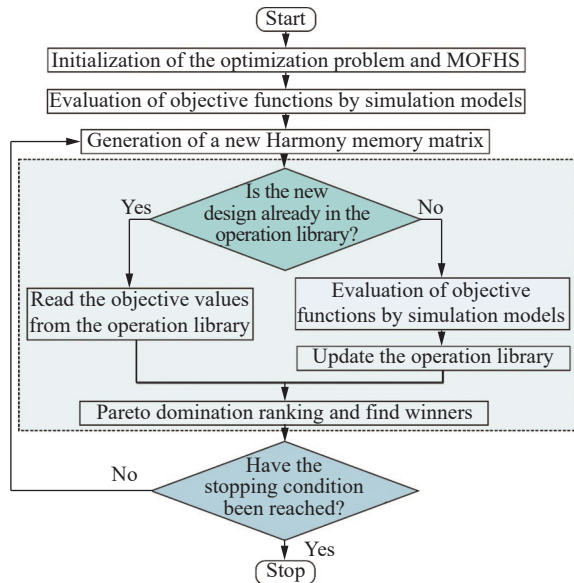


**Fig. 1** Flowchart of the MOSO model of optimal design of groundwater remediation system based on the MOFHS algorithm

Step I. Initialization of the optimization problem and the MOFHS algorithm

This step involves two primary tasks:

1. Establishing accurate simulation models for groundwater flow and contaminant transport. These models are used to define the objective functions and constraints of the MOSO model.

2. Initializing the MOFHS by setting control parameters and generating the initial population.

Step II. Evaluation of objective functions

Objective functions are evaluated by simulating the groundwater flow and contaminant transport. This involves obtaining the pumping volume and distribution of contaminant plume using the MODFLOW and MT3DMS programs.

Step III. Generation of a new harmony memory

A new harmony vector is generated based on the following three principles:

1. Memory consideration,
2. Pitch adjustment,
3. Random selection.

Step IV. Determination of the present Pareto optimal solutions

In this step, the algorithm identifies Pareto-optimal solutions using Pareto domination ranking and

Pareto solution set filter. Furthermore, an operation library of individual fitness is used to enhance the calculation speed of MOFHS.

Step V. Stopping condition judgement

The algorithm checks if the stopping condition has been met. If met, the iteration process of MOFHS is terminated. Otherwise, the program loops back to step II and continues.

## 2 Case study

### 2.1 2-D hypothetical example

#### 2.1.1 Description of the 2-D hypothetical example

The 2-D hypothetical example considers a homogeneous and isotropic aquifer divided into 16 rows and 20 columns, each with a step size of 40 meters (Zheng and Wang, 2003). It is assumed that the aquifer has been contaminated by an existing plume, as illustrated in Fig. 2. The aquifer's boundary conditions are: The east and west sides are constant head boundaries, with head values of 10 m on the west side and 8 m on the east side; the south and north sides are no-flow boundaries. For the transport model, the boundary conditions include: No mass flux on the west, north, and south sides, and specified advective mass flux on the east side (Zheng and Wang, 2003). The remediation target is to ensure that the calculated concentration at any monitoring point within the area of compliance remains below 2 mmol/L.

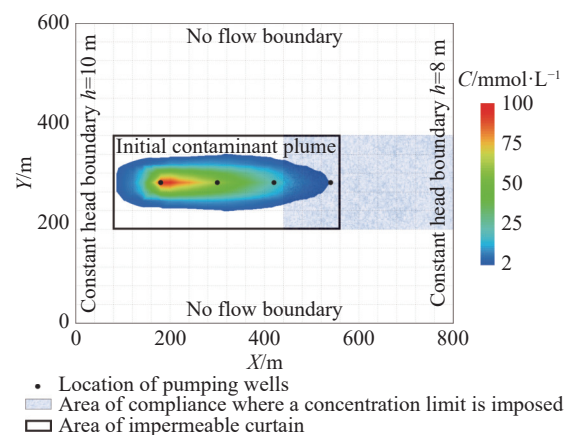


**Fig. 2** Configuration of the 2-D hypothetical example (modified from Zheng and Wang, 2003)

#### 2.1.2 Scenarios setting

Aquifers are generally classified into two main types: Confined aquifers and unconfined aquifers (Warren et al. 2002). In this study, these were designated as scenario 1 ( $S_1$ ) and scenario 2 ( $S_2$ ), respectively. The input parameters for the flow and

transport model in the 2-D hypothetical example are presented in Table 1.

**Table 1** Input parameters of flow and transport models for 2-D hypothetical example (Harbaugh AW and McDonald MG, 1996)

Parameters	Value
Specific yield (-)	0.2
Storage coefficient of S <sub>2</sub> (-)	10 <sup>-4</sup>
Aquifer thickness of S <sub>1</sub> (m)	5
Aquifer thickness of S <sub>2</sub> (m)	10
Average head of S <sub>1</sub> and S <sub>2</sub> (m)	9

The primary hydrogeological parameters influencing the remediation effect include hydraulic conductivity (*K*), porosity (*n*), and longitudinal dispersivity ( $\alpha_L$ ). The ratio of transverse dispersivity to longitudinal dispersivity was set at 0.2 (Liu et al. 2021). Various combinations of *K*, *n* and  $\alpha_L$  were used to simulate different hydrogeological conditions and contaminant characteristics. In addition, the remediation period ( $T_{re}$ ) was identified as a critical factor affecting the remediation outcomes. The impacts of *K*, *n*,  $\alpha_L$ , and  $T_{re}$  on the remediation effect were evaluated using Case1 to Case9, as detailed in Table 2.

**Table 2** Cases settings and parameters for S<sub>1</sub> and S<sub>2</sub>

Cases	Parameters			
	<i>K</i> (m/d)	<i>n</i> (-)	$\alpha_L$ (m)	$T_{re}$ (d)
Case1	1	0.2	50	365
Case2	5	0.2	50	365
Case3	10	0.2	50	365
Case4	5	0.1	50	365
Case5	5	0.3	50	365
Case6	5	0.2	25	365
Case7	5	0.2	100	365
Case8	5	0.2	50	180
Case9	5	0.2	50	730

**2.1.3 Results analysis and discussion**

In typical applications, impermeable curtains are constructed with uniform thickness, spanning the entire depth of the aquifer. To estimate the costs associated with impermeable curtains and the PAT system, inquiries were conducted through phone interviews and social media platforms involving over 100 wastewater treatment and impermeable curtains construction companies. These inquiries provided cost data for  $p_1$  (unit price for treating contaminated water) and  $p_2$  (unit price for constructing impermeable curtains). From the compiled data, the following conclusions were drawn:

(1) The unit price for PAT system ( $p_1$ ) is primarily determined by the characteristics of the water to be treated, such as its composition and specific remediation requirements. Since these factors remain consistent whether impermeable curtains are used or not, an average value of 100 was adopted for organically contaminated sites.

(2) The unit price for impermeable curtains ( $p_2$ ) is significantly influenced by factors such as material availability at the remediation site, transportation complexity, and construction techniques employed. These factors generally lead to price fluctuations within a range of  $\pm 50\%$  around an average value of 400.

Using the derived values of  $p_1$  and  $p_2$ , the total cost components of the remediation project,  $f_{PAT}$ ,  $f_{CIC}$  and  $f_T$ , for scenarios involving impermeable curtains were calculated based on Eqs. (1)-(5). The summarized results are presented in Table 3.

**Table 3** Calculation results of S<sub>1</sub> and S<sub>2</sub> under construction of impermeable curtains

Parameter	Value (S <sub>1</sub> )	Value (S <sub>2</sub> )
$p_1$ (CNY/m <sup>3</sup> )	100	100
$p_2$ (CNY/m <sup>2</sup> )	400 ( $\pm 50\%$ )	400 ( $\pm 50\%$ )
$Q$ ( $\times 10^5$ m <sup>3</sup> )	0.96	1.92
$f_{PAT}$ (Mio. CNY)	9.6	19.2
Area of impermeable curtain ( $\times 10^3$ m <sup>2</sup> )	6.8	13.6
$f_{CIC}$ (Mio. CNY)	1.36–4.08	2.72–8.16
$f_T$ (Mio. CNY)	10.96–13.68	21.92–27.36

Fig. 3 shows optimization results of groundwater remediation systems considering changes in *K* of aquifers. Each dot in the figure represents a Pareto optimal solution, which corresponds to an optimal design of the groundwater remediation system (the best combination of pumping rate for each pumping well). The Pareto solutions are categorized into the following three groups:

1. Optimal Solutions (OS):

These are the Pareto solutions located within the light blue area. OS represent solutions that lie below the minimum feasible value of the total remediation cost  $f_T$ ;

2. Potential Optimal Solutions (POS):

These are the Pareto solutions located within the light-yellow area. POS encompass solutions that fall between the minimum and maximum feasible values of  $f_T$ .

3. Unconsidered Solutions (US):

These are the Pareto solutions found in the light gray area. US includes solutions that exceed the maximum feasible value of  $f_T$  and, thus, are not considered viable for the optimization.

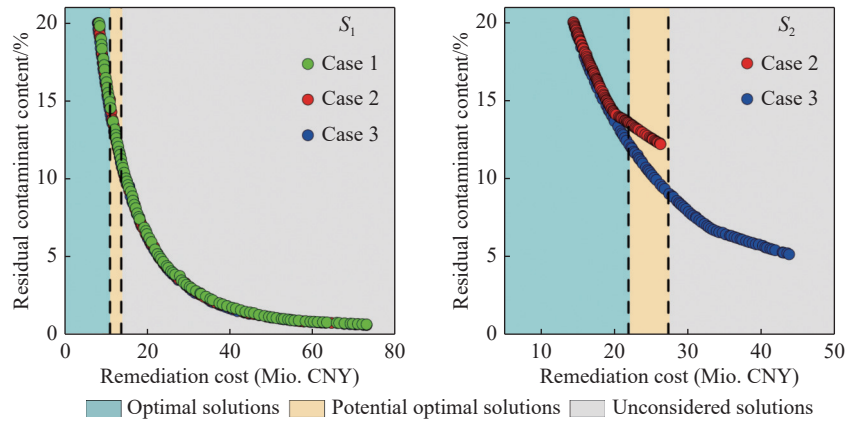


Fig. 3 Optimization results of  $S_1$  and  $S_2$  without impermeable curtains under different  $K$

The optimization results exhibit no significant difference in the performance of the groundwater remediation system when varying the hydraulic conductivity ( $K$ ) for confined aquifers. In contrast, for unconfined aquifers, changes in  $K$  significantly impact the optimization results. Notably, when the  $K$  value is 1 m/d, no optimization results are found. This occurs because, at this low permeability, the unconfined aquifer would be drained too easily by the PAT system. With the limited remediation time available, the PAT system is unable to identify any suitable remediation strategies that meet the remediation targets and constraints.

For unconfined aquifers, as  $K$  increase from 1 m/d to 10 m/d, the number of OS and pOS increases significantly. When  $K$  equals to 1 m/d,

even though no Pareto solutions are found, the transport of contaminant plume is restricted, with no contaminants migrating beyond the area protected by impermeable curtains (Fig. 4 case1). Therefore, under such conditions, constructing impermeable curtains becomes unnecessary.

Fig. 5 illustrates the optimization results of groundwater remediation systems, highlighting the significant impacts of  $n$  on the optimization results for both confined and unconfined aquifers. As the  $n$  value increases from 0.1 to 0.3, both OS and pOS gradually decrease. This trend occurs because an increase in  $n$  enhances the transport of contaminants making it more difficult to effectively capture and contain the contaminants. As a result, remediation costs increase.

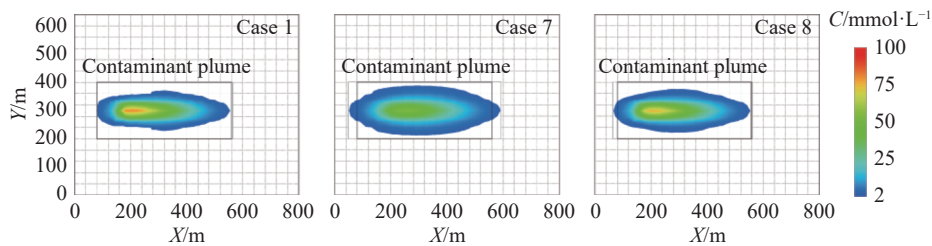


Fig. 4 The transport results of contaminant in case1, case7 and case8

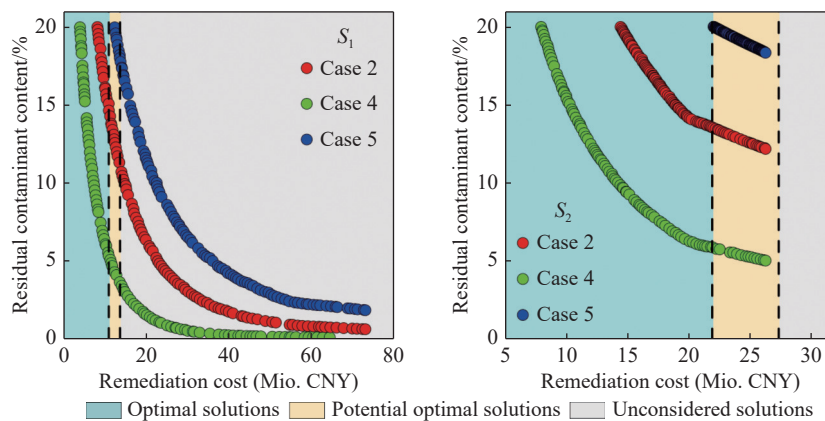


Fig. 5 Optimization results of  $S_1$  and  $S_2$  without impermeable curtains under different  $n$

For confined aquifers, the PAT system fails to identify any OS that meets the remediation target and constraint conditions when  $n$  increases to 0.3. In contrast, for unconfined aquifers, the proportion of pOS increases steadily with rising  $n$  values. Ultimately, when  $n$  equals 0.3, all solutions are classified as pOS. This underscores the need for a careful assessment of site-specific hydrogeological conditions before deciding to implement impermeable curtains for the remediation of unconfined aquifers, particularly those with high  $n$ .

Fig. 6 displays the optimization results of groundwater remediation systems, emphasizing the significant impact of  $\alpha_L$  on both confined and unconfined aquifers. As  $\alpha_L$  increase from 25 m to 100 m, both OS and pOS gradually decrease. This trend mirrors the effect of increased  $n$ , as a higher  $\alpha_L$  leads to a greater contaminant transport distance. This increased dispersion makes contaminant capture more difficult, resulting in higher remediation costs.

For confined aquifers, when  $\alpha_L$  reaches 100 m, the PAT system fails to identify any OS or pOS that meet the remediation target. Similarly, for unconfined aquifers with  $\alpha_L$  of 100 m, no Pareto

solutions are found. Additionally, in this scenario (shown in Fig. 4, case7), the contaminants spread beyond the area of potential impermeable curtains. Therefore, to the construction of impermeable curtains becomes necessary to contain the contaminants effectively.

Fig. 7 illustrates the optimization results of groundwater remediation systems, focusing on the impacts of varying  $T_{re}$  (remediation time). The effects of changing  $T_{re}$  on the optimization results are similar for both confined and unconfined aquifers. Specifically, a reduction in  $T_{re}$  leads to a decrease in the minimum achievable residual contaminant content by the PAT system. This occurs because shortening the  $T_{re}$  results in a proportional reduction in the total pumping capacity of the PAT system. Since the magnitude of this pumping capacity directly influences remediation efficacy, a shorter  $T_{re}$  results in less effective contaminant removal.

For confined aquifers, the PAT system achieves minimum residual contaminant contents of 3.62%, 0.62%, and 0.15% when  $T_{re}$  equals to 180d, 360d, and 720d, respectively. Notably, the existence of OS under all  $T_{re}$  implies that the construction of

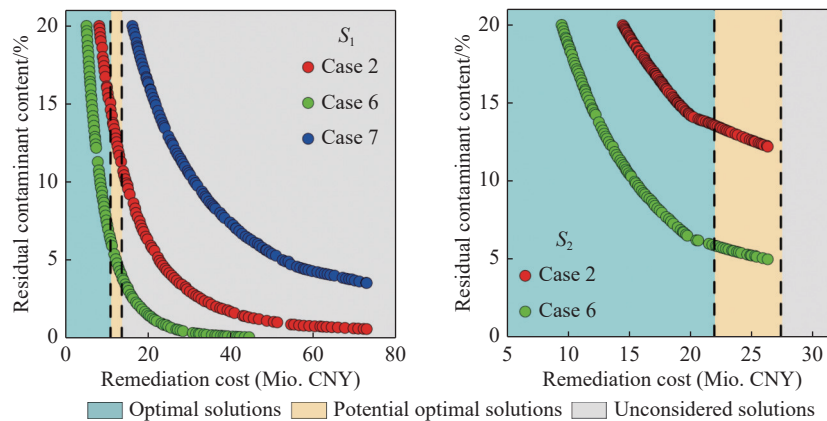


Fig. 6 Optimization results of  $S_1$  and  $S_2$  without impermeable curtains under different  $\alpha_L$

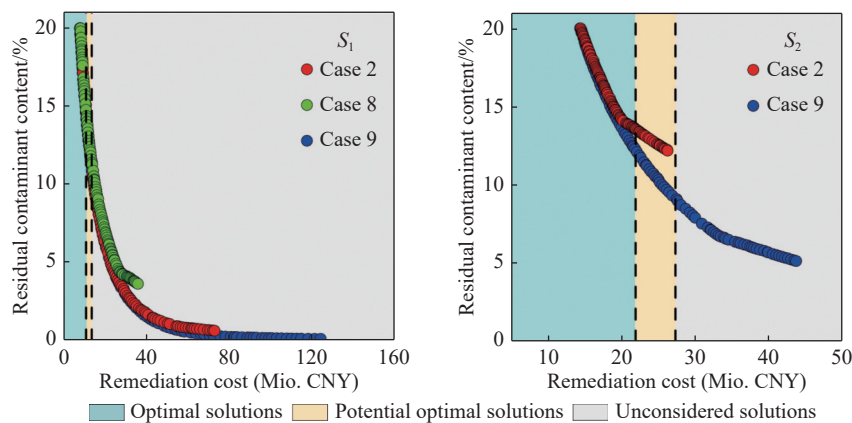


Fig. 7 Optimization results of  $S_1$  and  $S_2$  without impermeable curtains under different  $T_{re}$

impermeable curtains is unnecessary for confined aquifers.

In contrast, for unconfined aquifers, the PAT system achieves a minimum residual contaminant content of 34.81% with  $T_{re}$  of 180 days, which does not meet the constraint conditions. However, as  $T_{re}$  increases to 360 days and 720 days, the residual contaminant content decreases to 12.25% and 5.14%, respectively. Importantly, when  $T_{re}$  equals to 180 days, no Pareto solution exists for unconfined aquifers. As depicted in Fig. 4 (case8), contaminants will spread beyond the area of poten-

tial impermeable curtains, emphasizing the necessity of constructing impermeable curtains in advance for effective remediation.

### 2.2 3-D field example

The 3-D field application site in this study is based on an abandoned chemical plant located in Huai-bei, Anhui Province, China (Fig. 8(a)). The hydrogeological profile of the study area is depicted in Fig. 8(b). The groundwater system in the study area is modeled as a three-dimensional, homoge-

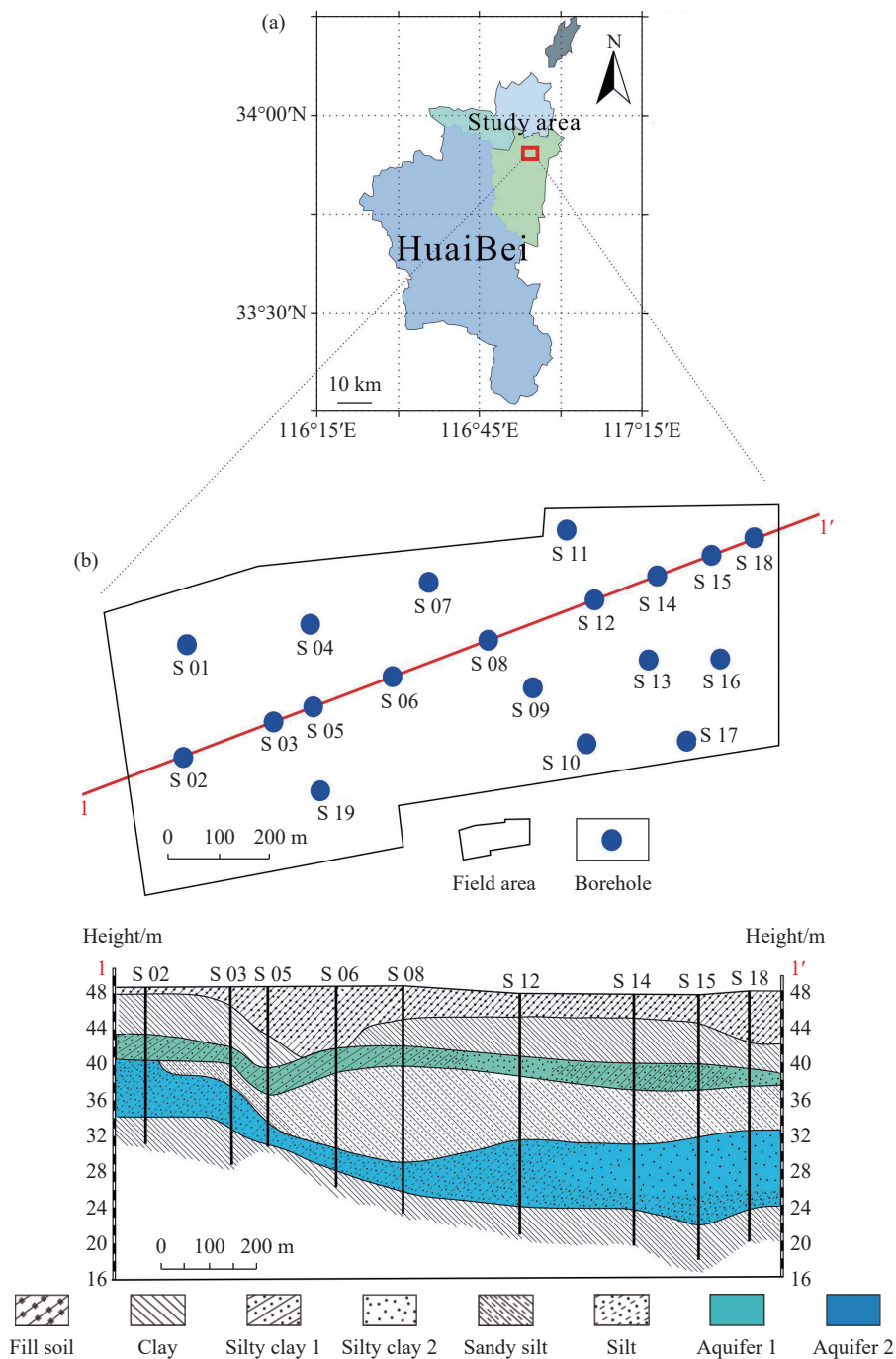


Fig. 8 (a) Geographical location of the study area. (b) Hydrogeological profile of the study area

neous, anisotropic transient flow system comprising two confined aquifers, named aquifer 1 (top) and aquifer 2 (bottom). The aquifers in the study area have been contaminated by benzene, which was deliberately selected as the target contaminant for this study. The initial contaminant plumes of benzene in aquifers are shown in Fig. 9(b), including the locations of pumping wells. Generally, Benzene in the aquifers exists in four primary states: Gaseous, adsorbed, dissolved and free-phase (Mercer and Cohen, 1990). The gaseous and adsorbed forms, along with free-phase benzene, primarily remain in the vadose zone and serve as potential sources of dissolved benzene upon their concentration depletion. Remediation efforts have already been carried out to address the gaseous, adsorbed and free-phase benzene in the aquifers. Consequently, this 3-D field problem is designed to focus specifically on the remediation of dissolved benzene in the aquifers, excluding any additional sources of contamination. The input parameters for the 3-D field problem are detailed in Table 4. The remediation target is to reduce the residual contaminant content in aquifers by the end of the  $T_{re}$  to below 20% of the initial contaminant concentration. Additionally, the concentrations at

all monitoring points within the region enclosed by impermeable curtains must remain below 120  $\mu\text{g/L}$ .

In the scenario where impermeable curtains are employed, the contaminated groundwater at the 3-D field site is contained by these curtains. As a result, the two key factors,  $f_{CIC}$  (site availability) and  $f_{PAT}$  (calculated by Eqs. (1)-(5)) are considered fixed constants. The total remediation cost for this scenario is 102 million Chinese Yuan (Mio. CNY).

The optimization results for remediation without impermeable curtains are shown in Fig. 9(a). As in the 2-D hypothetical example, an increase in remediation cost leads to a progressively slower reduction in residual contaminant content. However, the Pareto solutions in this scenario are located within the light green area, indicating that there are more cost-effective remediation strategies compared to when impermeable curtains are used. The remediation effects of one selected Pareto solution (solution 12) is shown in Fig. 9(c), demonstrating a cost-saving potential of approximately 38% compared to the remediation strategy involving impermeable curtains. The input parameters for the 3-D field example align with those of case1 in the 2-D hypothetical example for confined

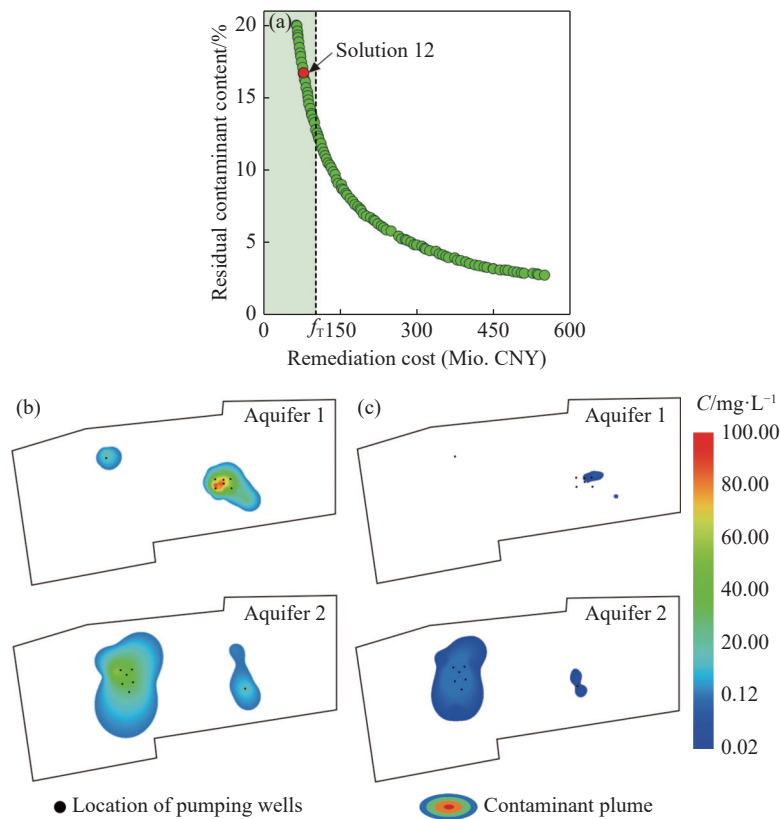


**Fig. 9** (a) Optimization results without impermeable curtains of the 3-D field example. (b) Initial contaminant plumes of aquifer 1 and aquifer 2. (c) Residual contaminant plumes of aquifer 1 and aquifer 2 under the remediation scheme of solution 12

**Table 4** Input parameters of the 3-D field example

Parameters	Value
Hydraulic conductivity of aquifer 1, 2 (m/d)	1.5
Porosity (-)	0.3
Specific yield (-)	0.2
Storage coefficient (-)	$10^{-4}$
Dispersivity (m)	20
Aquifer thickness of aquifer 1 (m)	3
Aquifer thickness of aquifer 2 (m)	8
Remediation period (d)	200

aquifers. Consequently, the optimization results obtained from the 3-D field example reinforce the findings from the 2-D example, further proving that impermeable curtains are not necessary for groundwater contaminant remediation projects.

### 3 Conclusion

This study primarily focuses on evaluating the necessity of impermeable curtains in groundwater contaminant remediation projects, using the PAT remediation technique as an example. This study provides calculation formulas for the total remediation cost involving impermeable curtains and compares these results with optimal Pareto solution derived from the MOSO framework without impermeable curtains.

The study utilizes a 2-D hypothetical example to simulate and assess key parameters that influence the optimization results, including  $K$ ,  $n$ ,  $\alpha_L$  and  $T_{re}$ . From this analysis, it is concluded that impermeable curtains should be constructed in cases where the  $\alpha_L$  of the contaminant is 100 m. In other scenarios, including those with aquifers of lower  $n$  (under 0.3), other more cost-effective and efficient remediation strategies are available, thus making impermeable curtains unnecessary. The findings from the 2-D hypothetical example are validated with a 3-D field example, further confirming that impermeable curtains are not essential in most cases. In these cases, alternative remediation strategies provide feasible, more cost-efficient, and effective options.

While the study provides valuable insights, there are several limitations. The study does not account for aquifers with unique features, particularly clay aquifers, which have high  $n$  values but pose challenges in terms of effective pumping. Furthermore, this study is centered on PAT as the primary technique. The necessity of constructing impermeable curtains should be re-evaluated for other remedia-

tion techniques in further studies, which may require a different approach.

### Acknowledgements

This research was financially supported by the National Key Research and Development Program of China (Grant No. 2022YFC3702200), the National Natural Science Foundation of China (Grant Nos.42372279 and U2267218), the Natural Science Foundation of Anhui Province (Grant No. JZ2022AKZR0451).

### References

- Bader J, Zitzler E. 2011. HypE: An algorithm for fast hypervolume-based many-objective optimization. *Evolutionary Computation*, 19: 45–76. DOI: [10.1162/EVCO\\_a\\_00009](https://doi.org/10.1162/EVCO_a_00009)
- Cao T, Zeng X, Wu J, et al. 2019. Groundwater contaminant source identification via Bayesian model selection and uncertainty quantification. *Hydrogeology Journal*, 27: 2907–2918. DOI: [10.1007/s10040-019-02055-3](https://doi.org/10.1007/s10040-019-02055-3).
- Chang LC, Chu HJ, Hsiao CT. 2007. Optimal planning of a dynamic pump-treat-inject groundwater remediation system. *Journal of Hydrology*, 342: 295–304. DOI: [10.1016/j.jhydrol.2007.05.030](https://doi.org/10.1016/j.jhydrol.2007.05.030).
- Deb K. 2001. Multi-Objective Optimization Using Evolutionary Algorithms: An Introduction. DOI: [10.1007/978-0-85729-652-8\\_1](https://doi.org/10.1007/978-0-85729-652-8_1).
- Deb K, Pratap A, Agarwal S, et al. 2002. A fast and elitist multiobjective genetic algorithm: NSGA-II. *IEEE Trans. Evolutionary Computation*, 6: 182–197. DOI: [10.1109/4235.996017](https://doi.org/10.1109/4235.996017).
- Elango L, Brindha K, Kalpana L, et al. 2012. Groundwater flow and radionuclide decay-chain transport modelling around a proposed uranium tailings pond in India. *Hydrogeology Journal*, 20: 797–812. DOI: [10.1007/s10040-012-0834-6](https://doi.org/10.1007/s10040-012-0834-6).
- Fu F, Dionysiou DD, Liu H. 2014. The use of zero-valent iron for groundwater remediation and wastewater treatment: A review. *Journal of Hazardous Materials*, 267: 194–205. DOI: [10.1016/j.jhazmat.2013.12.062](https://doi.org/10.1016/j.jhazmat.2013.12.062).
- Harbaugh, AW, ER Banta MC, Hill MG McDon-

- ald. 2000. MODFLOW-2000, the U. S. Geological Survey modular groundwater model—User guide to modularization concepts and the groundwater flow process. USGS Open-File Report 00–92. Reston, Virginia: USGS. (Open-File Report).
- Harbaugh AW, McDonald MG. 1996. Programmer's documentation for MODFLOW-96, an update to the U. S. Geological Survey Modular Finite-difference Groundwater Flow Model: U. S. Geological Survey Open-File Report: 96–486.
- Gao JH, Wang YS, Li YB, et al. 2019. Design of the dewatering project of pit with pensile curtains in the floodplain area near Yangtze River. *IOP Conference Series Earth and Environmental*, 376: 012062. DOI: [10.1088/1755-1315/376/1/012062](https://doi.org/10.1088/1755-1315/376/1/012062).
- Kim S, Lim H, Yoon S. 2017. A study on the impermeable effect by grouting in the Subsea Tunnel. *Journal of Korean Geo-Environmental Society*, 18: 5–19. DOI: [10.14481/JKGES.2017.18.6.5](https://doi.org/10.14481/JKGES.2017.18.6.5).
- Liu C, Chen X, Banwart SA, et al. 2021. A novel permeable reactive biobarrier for ortho-nitrochlorobenzene pollution control in groundwater: Experimental evaluation and kinetic modelling. *Journal of Hazardous Materials*, 420: 126563. DOI: [10.1016/j.jhazmat.2021.126563](https://doi.org/10.1016/j.jhazmat.2021.126563)
- Locatelli L, Binning PJ, Sanchez-Vila X, et al. 2019. A simple contaminant fate and transport modelling tool for management and risk assessment of groundwater pollution from contaminated sites. *Journal of Contaminant Hydrology*, 221: 35–49. DOI: [10.1016/j.jconhyd.2018.11.002](https://doi.org/10.1016/j.jconhyd.2018.11.002)
- Luo Q, Wu JF, Sun X, et al. 2012. Optimal design of groundwater remediation systems using a multi-objective fast harmony search algorithm. *Hydrogeology Journal*, 20: 1497–1510. DOI: [10.1007/s10040-012-0900-0](https://doi.org/10.1007/s10040-012-0900-0)
- Luo Q, Wu JF, Yang Y, et al. 2016. Multi-objective optimization of long-term groundwater monitoring network design using a probabilistic Pareto genetic algorithm under uncertainty. *Journal of Hydrology*, 534: 352–363. DOI: [10.1016/j.jhydrol.2016.01.009](https://doi.org/10.1016/j.jhydrol.2016.01.009).
- Luo Q, Wang JF, Yang Y, et al. 2014. Optimal design of groundwater remediation system using a probabilistic multi-objective fast harmony search algorithm under uncertainty. *Journal of Hydrology*, 519: 3305–3315. DOI: [10.1016/j.jhydrol.2014.10.023](https://doi.org/10.1016/j.jhydrol.2014.10.023).
- Luo Q, Yang Y, Qian J, et al. 2020. Spring protection and sustainable management of groundwater resources in a spring field. *Journal of Hydrology*, 582: 124498. DOI: [10.1016/j.jhydrol.2019.124498](https://doi.org/10.1016/j.jhydrol.2019.124498).
- Lyu HM, Shen SL, Wu YX, et al. 2021. Calculation of groundwater head distribution with a close barrier during excavation dewatering in confined aquifer. *Geoscience Frontiers*, 12: 791–803. DOI: [10.1016/j.gsf.2020.08.002](https://doi.org/10.1016/j.gsf.2020.08.002)
- Mattila V, Virtanen K. 2014. Maintenance scheduling of a fleet of fighter aircraft through multi-objective simulation-optimization. *Simulation*, 90: 1023–1040. DOI: [10.1177/0037549714540008](https://doi.org/10.1177/0037549714540008)
- Mercer JW, Cohen RM. 1990. A review of immiscible fluids in the subsurface: Properties, models, characterization and remediation. *Journal of Contaminant Hydrology*, 6: 107–163. DOI: [10.1016/0169-7722\(90\)90043-G](https://doi.org/10.1016/0169-7722(90)90043-G).
- Park YC. 2016. Cost-effective optimal design of a pump-and-treat system for remediating groundwater contaminant at an industrial complex. *Geosciences Journal*, 20: 891–901. DOI: [10.1007/s12303-016-0030-0](https://doi.org/10.1007/s12303-016-0030-0).
- Rao SS. 1979. Optimization—theory and applications. *International Journal for Numerical Methods in Engineering*. DOI: [10.1002/nme.1620141118](https://doi.org/10.1002/nme.1620141118).
- Rodell M, Velicogna I, Famiglietti JS. 2009. Satellite-based estimates of groundwater depletion in India. *Nature*, 460: 999–1002. DOI: [10.1038/nature08238](https://doi.org/10.1038/nature08238).
- Song J, Yang Y, Chen G, et al. 2019. Surrogate assisted multi-objective robust optimization for groundwater monitoring network design. *Journal of Hydrology*, 577: 123994. DOI: [10.1016/j.jhydrol.2019.123994](https://doi.org/10.1016/j.jhydrol.2019.123994).
- Song J, Yang Y, Wu JF, et al. 2018. Adaptive surrogate model based multiobjective optimization for coastal aquifer management. *Journal of Hydrology*, 561: 98–111. DOI: [10.1016/j.jhydrol.2018.03.063](https://doi.org/10.1016/j.jhydrol.2018.03.063).
- Song YC. 2014. Research for seepage prevention type of dam foundation of Xiabandi hydraulic

- engineering in Xinjiang. *Applied Mechanics and Materials*, 501–504: 1942–1946. DOI: [10.4028/www.scientific.net/AMM.501-504.1942](https://doi.org/10.4028/www.scientific.net/AMM.501-504.1942).
- Tang Z, Song L, Jin D, et al. 2023. An engineering case history of the prevention and remediation of sinkholes induced by limestone quarrying. *Sustainability*, 15: 2808. DOI: [10.3390/su15032808](https://doi.org/10.3390/su15032808).
- Vidic RD, Brantley SL, Vandenbossche JM, et al. 2013. Impact of shale gas development on regional water quality. *Science*, 340: 1235009. DOI: [10.1126/science.1235009](https://doi.org/10.1126/science.1235009).
- Wang N, Wang Q, Ye WM, et al. 2024. Research progress of microbial reinforcement technology. *Hydrogeology & Engineering Geology*, 51(5): 231–244. DOI: [10.16030/j.cnki.issn.1000-3665.202401013](https://doi.org/10.16030/j.cnki.issn.1000-3665.202401013).
- Wang Z, Li W, Li Z, et al. 2020. Groundwater response to oil storage in large-scale rock caverns with a water curtain system: Site monitoring and statistical analysis. *Tunnelling and Underground Space Technology*, 99: 103363. DOI: [10.1016/j.tust.2020.103363](https://doi.org/10.1016/j.tust.2020.103363)
- Wang Z, Yang Y, Wu JF, et al. 2022. Multi-objective optimization of the coastal groundwater abstraction for striking the balance among conflicts of resource-environment-economy in Longkou City, China. *Water Resource*, 211: 118045. DOI: [10.1016/j.watres.2022.118045](https://doi.org/10.1016/j.watres.2022.118045)
- Warren V, Gary L, John W. 2002. *Introduction to Hydrology*.
- Wu J, Zheng C, Chien CC. 2005. Cost-effective sampling network design for contaminant plume monitoring under general hydrogeological conditions. *Journal of Contaminant Hydrology*. 77: 41–65. DOI: [10.1016/j.jconhyd.2004.11.006](https://doi.org/10.1016/j.jconhyd.2004.11.006)
- Yang K, Xu C, Chi M, et al. 2022. Analytical analysis of the groundwater drawdown difference induced by foundation pit dewatering with a suspended waterproof curtain. *Applied Sciences*, 12: 10301. DOI: [10.3390/app122010301](https://doi.org/10.3390/app122010301).
- Yang Y, Luo Q, Ye G. 2018. Optimization of water allocation system at the river basins. Presented at the 14th International Conference on Natural Computation, Fuzzy Systems and Knowledge Discovery (ICNC-FSKD).
- Yang Y, Song J, Simmons CT, et al. 2021. A conjunctive management framework for the optimal design of pumping and injection strategies to mitigate seawater intrusion. *Journal of Environmental Management*, 282: 111964. DOI: [10.1016/j.jenvman.2021.111964](https://doi.org/10.1016/j.jenvman.2021.111964).
- Yang Y, Wu JF, Luo Q, et al. 2017. Effects of stochastic simulations on multiobjective optimization of groundwater remediation design under uncertainty. *Journal of Hydrologic Engineering*, 22: 04017015. DOI: [10.1061/\(ASCE\)HE.19435584.0001510](https://doi.org/10.1061/(ASCE)HE.19435584.0001510).
- Zheng C, Wang PP. 2003. *A modular groundwater optimizer incorporating MODFLOW/MT3DMS. Documentation and user's guide*. University of Alabama and Groundwater Systems Research Ltd. Tuscaloosa, AL.
- Zheng C, Wang PP. 1999. *MT3DMS: A modular three-dimensional multispecies transport model for simulation of advection, dispersion, and chemical reactions of contaminants in groundwater systems. Documentation and User's Guide*. Contract Report SERDP-99-1. US Army Engineer Research and Development Center, Vicksburg, Mississippi, USA: 202.
- Zong WG, Joong HK, Loganathan GV. 2001. A new heuristic optimization algorithm: Harmony search. *Simulation*, 76: 60–68. DOI: [10.1177/003754970107600201](https://doi.org/10.1177/003754970107600201).